Two-Dimensional QSAR Studies on Arylpiperazines as High-Affinity 5-HT_{1A} Receptor Ligands

Karen C. Weber[1], Káthia M. Honório[2], Adriano D. Andricopulo[3] and Albérico B. F. Da Silva[1,*]

[1]*Instituto de Química de São Carlos, Universidade de São Paulo, Av. Trabalhador São-Carlense, 400, 13560-970, São Carlos, SP, Brazil;* [2]Escola de Artes, Ciências e Humanidades, Universidade de São Paulo, Av. Arlindo Bettio, 1000, 03828-000, São Paulo, SP, Brazil; [3]*Laboratório de Química Medicinal e Computacional, Centro de Biotecnologia Molecular Estrutural, Instituto de Física de São Carlos, Universidade de São Paulo, Av. Trabalhador São-Carlense, 400, 13560-970, São Carlos, SP, Brazil*

Abstract: 5-HT_{1A} receptor plays an important role in the delayed onset of antidepressant action of a class of selective serotonin reuptake inhibitors. Moreover, 5-HT_{1A} receptor levels have been shown to be altered in patients suffering from major depression. In this work, hologram quantitative structure–activity relationship (HQSAR) studies were performed on a series of arylpiperazine compounds presenting affinity to the 5-HT_{1A} receptor. The models were constructed with a training set of 70 compounds. The most significant HQSAR model (q^2 = 0.81, r^2 = 0.96) was generated using atoms, bonds, connections, chirality, and donor and acceptor as fragment distinction, with fragment size of 6–9. Predictions for an external test set containing 20 compounds are in good agreement with experimental results showing the robustness of the model. Additionally, useful information can be obtained from the 2D contribution maps.

Key Words: HQSAR, arylpiperazines, 5-HT_{1A} receptor, SSRIs, drug design.

1. INTRODUCTION

The serotonin system has long been implicated in the etiology of many disorders such as depression, schizophrenia, migraine, suicidal behavior, infantile autism, eating and obsessive compulsive disorders. Particularly, in cases of depression, the availability of antidepressants with a faster onset of action is a therapeutic aim to be achieved. This is due to the fact that selective serotonin reuptake inhibitors (SSRIs) achieve their therapeutic effects only after repeated administration [1-5].

It has been shown that the 2- to 6-week latency period for the SSRIs begin to exert their clinical effects is related to the regulatory role of 5-HT_{1A} autoreceptors, which inhibit the firing rate of serotonergic neurons [6,7]. This assumption is mainly supported by studies showing that pindolol, a 5-HT_{1A} receptor antagonist, is able to accelerate the antidepressant action of SSRIs in several open and placebo controlled clinical trials [8-11]. Furthermore, alterations in 5-HT_{1A} receptor levels are reported in depression and suicide, and gene knockout of the 5-HT_{1A} receptor results in an anxiety phenotype, suggesting that abnormal transcriptional regulation of this receptor gene may underlie these disorders [12,13].

In the search for novel antidepressant agents, Monge and co-workers [14-17] have investigated new compounds with a dual mode of action, that is, serotonin reuptake inhibition and 5-HT_{1A} receptor antagonism. The strategy employed a combination of two chemically distinct frameworks (associated to the sought activities) in a single chemical entity. The drug design was based on coupling of the selected pharmacophores close related to the corresponding inhibition of serotonin reuptake (e.g., benzocondensed, fluorophenyl rings) to arylpiperazines, which are typical 5-HT_{1A} receptor ligands. The analyses of different Z, Ar_1 and Ar_2 groups (Fig. **1**) allowed the identification of important structure-activity relationships regarding 5-HT_{1A} binding affinity. For example, when Z was a CHOH group instead CO or other bulky groups, the compounds showed improved affinity; ortho-substitution or the presence of a heteroatom at Ar_1 were favorable for 5-HT_{1A} receptor binding. Affinity enhancements were also obtained when a phenyl ring in Ar_2 was replaced by thiophene, and when a naphthalene group was replaced by benzothiophene [16,17]. These results are in agreement with studies on different arylpiperazine derivatives which indicated that a n=4 chain between Ar_2 and N1 (Fig. **1**) is an important factor for optimal 5-HT_{1A} binding [18,19].

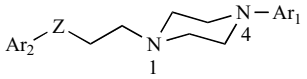

Fig. (1). General structure of arylpiperazines.

Despite the available SAR information on arylpiperazines, only a very few quantitative models relating structure to 5-HT_{1A} receptor affinity can be found in the literature [20-25]. In order to investigate the quantitative structure-activity relationships (QSAR) of a large series of selected arylpiperazine derivatives as 5-HT_{1A} receptor ligands, we have employed the hologram QSAR (HQSAR) method. HQSAR is a 2D QSAR technology which explains differences in the observed activity in a series of molecules by quantifying variations within their calculated molecular holograms using the partial least squares (PLS) method. HQSAR can be applied to large data sets of structures, as well as traditional small-

*Address correspondence to this author at the Instituto de Química de São Carlos, Universidade de São Paulo, Av. Trabalhador São-Carlense, 400, 13560-970, São Carlos, SP, Brazil; Tel/Fax: +55 (16) 3373 9975;
E-mail: alberico@iqsc.usp.br

1573-4064/08 $55.00+.00

size data sets. The statistical results produced with HQSAR are comparable in quality to 3D QSAR techniques, such as CoMFA, with the advantage of eliminating the need of bioactive conformation selection and 3D molecular alignment [26-29].

2. METHODOLOGY

2.1. Computational Approach

The modeling analyses, calculations, and visualizations for HQSAR were performed using the SYBYL 7.2 package (Tripos Inc., St. Louis, USA) running on Red Hat Enterprise Linux workstations. A statistical cluster analysis was carried out with Tsar 3D version 3.3 (Accelrys, San Diego, USA) employing the complete linkage clustering method with no standardization as previously described [30,31].

2.2. Data Set Characterization

The data set used for the HQSAR analyses consists of a series of 90 arylpiperazines with affinity at the 5-HT_{1A} receptor [16,17]. The chemical structures and corresponding biological property for the complete set of compounds are listed in Table **1**. The structures of the bioactive compounds were constructed using the Concord tool available in the molecular modeling software package SYBYL 7.2.

2.3. HQSAR Analysis

Statistical HQSAR modeling was carried out as previously described [28-31]. Briefly, HQSAR requires only 2D structures and biological activity as input. In this method, each molecule in the data set is broken down into several unique structural fragments, which are arranged to form a molecular hologram, encoding all possible molecular fragments (i.e., linear, branched, and overlapping). With the transformation of the chemical representation of a molecule into its corresponding molecular hologram, this method requires no explicit 3D information for the ligands. However, the process of incorporating information about each fragment, and each of its constituent subfragments, implicitly encodes 3D structural information (i.e., hybridization state of each carbon atom, stereochemistry of one or more chiral centers). HQSAR models can be affected by a number of parameters concerning hologram generation: hologram length, fragment size, and fragment distinction. Several combinations of fragment distinction were considered during the QSAR modeling runs. Holograms were generated with the standard parameters implemented in SYBYL 7.2 using distinct combinations of the following fragment distinction: atoms (A), bonds (B), connections (C), hydrogen atoms (H), chirality (Ch), and donor and acceptor (DA). HQSAR analyses were performed by screening the 12 default series of hologram lengths values from 53 to 401 bins. The patterns of fragment counts from the training set compounds were then related to the experimental biological activity. HQSAR models generated in our studies were investigated using full cross-validated correlation coefficient (q^2) with PLS Leave-One-Out (LOO) method.

3. RESULTS AND DISCUSSION

The HQSAR models were derived for a series of 90 arylpiperazines as high affinity ligands of the 5-HT_{1A} receptor. The values of K_i employed in this work vary from 1.9 to 5000 nM (a factor of about 2600) and are acceptably distributed across the range of values. The *in vitro* K_i values were converted into the corresponding pK_i (-log K_i) values for modeling purposes. It is worth noting that the K_i values used in this work were measured under the same experimental conditions [16,17], a fundamental requirement for the creation of reliable QSAR models. The selection of appropriate training and test sets is also of critical importance in QSAR studies. With the assistance of the program Tsar 3D, the original data set of 90 compounds was divided into training set (compounds **1**–**70**, Table **1**) for model construction, and test set (compounds **71-90**, Table **1**) for external model validation, in such a way that structurally diverse molecules possessing activities (K_i) of a wide range were included in both sets. This data set was selected both because the compounds provide an appropriate structural diversity for QSAR modeling and because the availability of high quality biological data. Thus, the data set created is suitable for QSAR model development.

In order to better understand the quantitative nature of the structure-activity relationships involved in this data set of arylpiperazines, we have conducted 2D QSAR studies using the HQSAR method. HQSAR investigation requires selecting values for parameters that specify the length of the hologram, as well as the size and type of fragment that are to be encoded. Initially, the molecular fragments were obtained using the following fragment distinctions: atoms (A), bonds (B), connections (C), hydrogen atoms (H), chirality (Ch), and donor and acceptor (DA). Several combinations of these parameters were considered using the fragment size default (4-7) as follows: A/B, A/B/C, A/B/C/H, A/B/C/H/Ch, A/B/C/H/Ch/DA, A/B/H, A/B/C/Ch, A/B/DA, A/B/C/DA, A/B/H/DA, A/B/C/Ch/DA, A/B/C/H/DA, and A/B/H/Ch/DA. HQSAR analyses were performed over the 12 default series of hologram lengths of 53, 59, 61, 71, 83, 97, 151, 199, 257, 307, 353, and 401 bins. The statistical results from the PLS analyses for the 70 training set compounds using the several fragment distinction combinations are listed in Table **2**.

The results in Table **2** indicate the good quality of the models obtained using different combinations of fragment distinction. The best statistical results among all models were obtained for model 11 ($q^2 = 0.76$, $r^2 = 0.93$). This model was derived using the combination of atoms, bonds, connections, chirality, and donor and acceptor, with 6 being the optimum number of PLS components. This implicates an important role of structure-activity relationships in the generation of the HQSAR models for this series of ligands. For this reason, independently of the data set under investigation, it is indispensable to assess the many different combinations of fragment distinction as well as fragment size in order to select the best statistical model [24-29].

The influence of different fragment sizes in the statistical parameters was further investigated for the best HQSAR model generated in Table **2** (model 11). Fragment size parameters control the minimum and maximum length of fragments to be included in the hologram fingerprint. The HQSAR results for the different fragment sizes used are summarized in Table **3**. The results show a considerable improvement in

Table 1. Chemical Structures and pK_i Values for the Series of Arylpiperazines Studied

Training Set Compounds					
Cpd	**General Structure**	**R**	**Z**	**Ar_1**	**K_i (nM)**
1	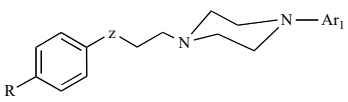	H	CHOH	2-methoxyphenyl	47.5
2		H	CHO-4-$CF_3C_6H_4$	2-methoxyphenyl	450
3		H	CHO-4-$CH_3OC_6H_4$	2-methoxyphenyl	90
4		H	CHO-3,4-$OCH_2OC_6H_3$	2-methoxyphenyl	20
5		H	CNOH	2-methoxyphenyl	17.5
6		H	CO	4-chlorophenyl	800
7		H	CHOH	4-chlorophenyl	800
8		H	CHO-4-$CF_3C_6H_4$	4-chlorophenyl	>5000
9		H	CHO-4-$CH_3C_6H_4$	4-chlorophenyl	1450
10		H	CNOH	4-chlorophenyl	>5000
11		H	CHOH	4-methoxyphenyl	>5000
12		H	CHOH	2-pyrimidyl	375
13		H	CHO-4-$CF_3C_6H_4$	2-pyrimidyl	1600
14		H	CO	2-chlorophenyl	180
15		H	CHOH	2-chlorophenyl	115
16		H	CO	4-fluorophenyl	800
17		H	CHOH	4-fluorophenyl	145
18		H	CHO-4-$CF_3C_6H_4$	4-fluorophenyl	>5000
19		H	CO	2-pyridyl	50
20		H	CHOH	2-pyridyl	155
21		H	CO	4-nitrophenyl	>5000
22		H	CHOH	4-nitrophenyl	>5000
23		phenyl	CHO-4-$CF_3C_6H_4$	2-methoxyphenyl	>5000
24		methoxy	CHOH	2-methoxyphenyl	325
25		methoxy	CHO-4-$CF_3C_6H_4$	2-methoxyphenyl	1000
26		nitro	CO	2-methoxyphenyl	50
27		nitro	CHOH	2-methoxyphenyl	10
28	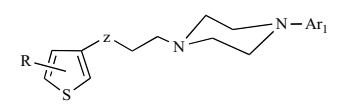	H	CO	2-methoxyphenyl	16
29		H	CHOH	2-methoxyphenyl	50
30		H	CHO-3,4-$OCH_2OC_6H_3$	2-methoxyphenyl	55
31		H	CHO-1-$C_{10}H_7$	2-methoxyphenyl	180
32		H	CNOH	2-methoxyphenyl	6.5
33		H	CO	4-chlorophenyl	700
34		H	CHOH	2-chlorophenyl	200
35		H	CO	1-naphthyl	35

(Table 1. Contd….)

Training Set Compounds					
Cpd	**General Structure**	**R**	**Z**	**Ar_1**	**K_i (nM)**
36		2,5-dimethyl	CO	2-methoxyphenyl	5
37		2,5-dimethyl	CHOH	2-methoxyphenyl	12
38		2,5-dimethyl	CO	2-hydroxyphenyl	7.5
39		2,5-dimethyl	CO	4-chloro-2-methoxyphenyl	500
40	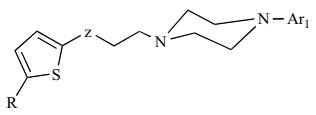	H	CHO-1-$C_{10}H_7$	2-methoxyphenyl	220
41		H	CO	4-chlorophenyl	>5000
42		H	CHOH	4-chlorophenyl	>5000
43		5-methyl	CO	2-methoxyphenyl	17.5
44		5-methyl	CHOH	2-methoxyphenyl	34
45	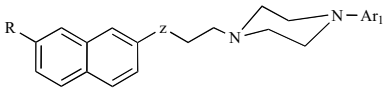	H	CO	2-methoxyphenyl	250
46		H	CHOH	2-methoxyphenyl	420
47		H	CO	4-chlorophenyl	>5000
48		H	CHOH	4-chlorophenyl	>5000
49		H	CHOH	2-hydroxyphenyl	190
50	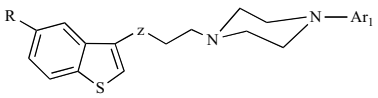	H	CHOH	2-methoxyphenyl	20
51		H	CNOH	2-methoxyphenyl	60
52		H	CO	4-chlorophenyl	>5000
53		H	CHOH	4-chlorophenyl	>5000
54		H	CO	2-hydroxyphenyl	110
55		H	CO	4-fluoro-2-methoxyphenyl	500
56		H	CHOH	4-fluoro-2-methoxyphenyl	500
57		H	CO	1-naphthyl	100
58		H	CHOH	1-naphthyl	66.7
59		H	CHOH	3-quinolyl	995
60		H	CHOH	5-quinolyl	36.8
61		H	CHOH	6-quinolyl	546
62		H	CHOH	8-quinolyl	6.3
63		H	CHOH	8-quinaldinyl	10.2
64		H	CHOH	4-indolyl	5.5
65		H	CHOH	3,4-dihydro-2H-1,5-benzo[*b*]dioxepin-6-yl	1.9
66		H	CHOH	5-benzo[*b*]thiophenyl	913
67		F	CHOH	1-naphthyl	2.7
68		F	CHOH	8-quinaldinyl	2.5
69		F	CHOH	4-indolyl	5.9
70		F	CHOH	3,4-dihydro-2H-1,5-benzo[*b*]dioxepin-6-yl	3

(Table 1. Contd….)

Training Set Compounds					
Cpd	**General Structure**	**R**	**Z**	**Ar_1**	**K_i (nM)**
71	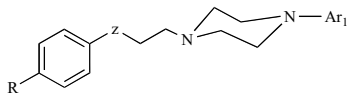	H	CO	2-methoxyphenyl	50
72		H	CHO-3,4-$OCH_2OC_6H_3$	4-chlorophenyl	550
73		H	CHO-4-$CF_3C_6H_4$	4-methoxyphenyl	>5000
74		H	CO	2-pyrimidyl	120
75		H	CHO-4-$CF_3C_6H_4$	2-chlorophenyl	>5000
76		H	CHO-4-$CF_3C_6H_4$	2-pyridyl	1600
77		H	CHO-4-$CF_3C_6H_4$	4-nitrophenyl	>5000
78	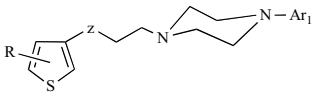	H	CHO-4-$CF_3C_6H_4$	2-methoxyphenyl	255
79		H	CHOH	4-chlorophenyl	2750
80		H	CO	2-chlorophenyl	200
81		2,5-dimethyl	CHOH	2-hydroxyphenyl	90
82	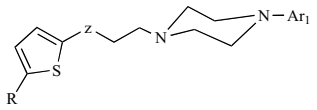	H	CO	2-methoxyphenyl	10
83		H	CHOH	2-methoxyphenyl	19
84	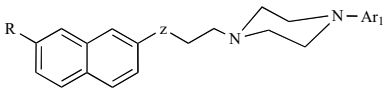	H	CO	2-hydroxyphenyl	1000
85	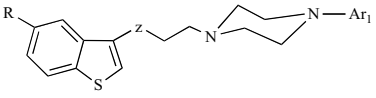	H	CO	2-methoxyphenyl	44
86		H	CHOH	2-hydroxyphenyl	18
87		H	CO	4-chloro-2-methoxyphenyl	500
88		H	CHOH	4-chloro-2-methoxyphenyl	361
89		H	CHOH	2,3-dihydro-1,4-benzodioxin-5-yl	5.7
90		F	CHOH	2,3-dihydro-1,4-benzodioxin-5-yl	6

Table 2. Results of HQSAR Analyses for Various Fragment Distinctions on the Key Statistical Parameters Using Fragment Size Default (4-7)

Model	Fragment Distinction	q^2	r^2	SEE	HL	*N*
1	A/B	0.60	0.80	0.48	61	6
2	A/B/C	0.57	0.86	0.41	257	6
3	A/B/C/H	0.59	0.83	0.45	353	6
4	A/B/C/H/Ch	0.58	0.85	0.42	71	6
5	A/B/C/H/Ch/DA	0.70	0.90	0.35	97	6
6	A/B/H	0.58	0.80	0.48	53	6
7	A/B/C/Ch	0.60	0.84	0.43	83	6
8	A/B/DA	0.68	0.91	0.33	401	6

(Table 2. Contd….)

Model	Fragment Distinction	q^2	r^2	SEE	HL	*N*
9	A/B/C/DA	0.66	0.91	0.33	307	6
10	A/B/H/DA	0.68	0.84	0.43	53	6
11	A/B/C/Ch/DA	0.76	0.93	0.28	307	6
12	A/B/C/H/DA	0.64	0.83	0.45	307	6
13	A/B/H/Ch/DA	0.60	0.76	0.52	53	4

q^2, cross-validated correlation coefficient; r^2, noncross-validated correlation coefficient; SEE, noncross-validated standard error; HL, hologram length; *N,* optimal number of components. Fragment Distinction: A, atoms; B, bonds; C, connections; H, hydrogen atoms; Ch, chirality; DA, donor and acceptor.

Table 3. Influence of Fragment Size on the Key Statistical Parameters Using the Best Fragment Distinction (Atoms, Bonds, Connections, Chirality, Donor and Acceptor)

Fragment Size	q^2	r^2	SEE	HL	*N*
2-5	0.69	0.89	0.36	199	6
3-6	0.71	0.92	0.31	257	6
4-7	0.76	0.93	0.28	307	6
5-8	0.79	0.95	0.24	257	6
6-9	0.81	0.96	0.22	353	6
7-10	0.78	0.93	0.26	353	6

Table 4. Experimental and Predicted Activities (pK_i) with Residual Values for the 20 Test Set Compounds

Test Set Compounds	pK_i		
	Experimental	Predicted	Residual[†]
71	5.56	5.74	0.18
72	8.24	8.61	0.37
73	7.74	7.02	-0.72
74	6.00	6.50	0.50
75	6.30	5.63	-0.67
76	7.05	7.28	0.23
77	5.80	5.68	-0.12
78	6.44	5.63	-0.81
79	6.70	6.61	-0.09
80	7.36	7.43	0.07
81	8.22	7.92	-0.30
82	6.92	7.14	0.22
83	6.26	6.46	0.20
84	7.30	7.27	-0.03
85	8.00	7.75	-0.25
86	7.72	6.91	-0.81
87	6.59	6.4	-0.19
88	5.30	5.24	-0.06
89	5.30	5.58	0.28
90	5.30	5.18	-0.12

[†]The difference between predicted and experimental values.

the statistical parameters (q^2 = 0.81, r^2 = 0.96) of the HQSAR model generated with fragment size 6-9.

The q^2 PLS LOO procedure used in the generation of the QSAR models may provide a suitable representation of the internal consistency and predictive ability of the best model for novel ligands. However, in order to assess its real predictive power, the best HQSAR model derived using the 70 training set molecules was assessed by predicting pK_i values for 20 test set molecules (compounds **71**–**90**, Table **1**), which were completely excluded during the training of the model. The results are shown in Table **4**, and the graphic results for the experimental versus predicted activities of both training set and test set are displayed in Fig. (**2**).

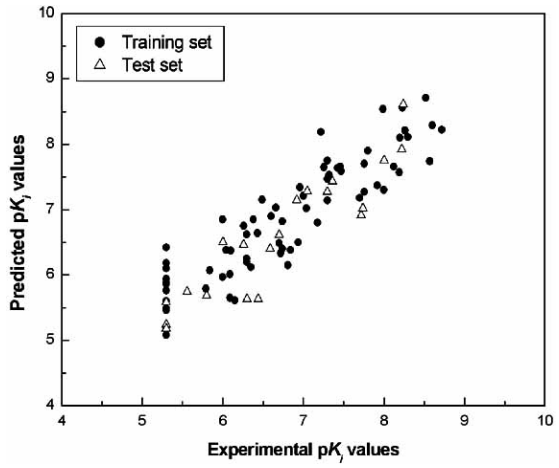

Fig. (2). Plot of predicted versus experimental values of pK_i for the training and test arylpiperazine compounds.

The good agreement between experimental and predicted values for the test set compounds indicates the reliability of the constructed HQSAR model. From the moderate/low residual values, it can be seen that the HQSAR model obtained is of sufficient quality to predict the biological potency of novel compounds within this structural class. The results show that the test set compounds, which represent the different structural properties incorporated within the training set, are well predicted without any outliers. The predicted values fall close to the experimental pK_i values, deviating by less than 0.40 log units in the majority of the cases. The only exceptions are compounds **73**, **74**, **75**, **78** and **86**, for which the predicted values are more substantial in error (between 0.50 and 0.81 log units).

Following the development of predictive statistical models for untested compounds, HQSAR can also be applied in drug design to provide useful hints about what molecular fragments are directly related to biological activity. This information, combined with knowledge of synthetic chemistry, could lead to the synthesis of new molecules with improved properties. In HQSAR, it is possible to visualize the individual atomic contributions to biological activity in a given molecule of the data set through the generation of contribution maps. The HQSAR module implemented in SYBYL 7.2 uses a color code in order to discriminate the main atomic contributions to biological activity. The colors at the red end of the spectrum (red, red orange and orange) indicate poor contributions, whereas colors at the green end (yellow, green blue and green) reflect favorable contributions. Atoms with intermediate contributions are colored white. In this way, the contribution map for the compound with higher (**65**, pK_i = 8.72) 5-HT$_{1A}$ receptor affinity was obtained as shown in Fig. (**3**). The fragments around the piperazine and thiophene rings are suggested as favorable contributions for 5-HT$_{1A}$ receptor affinity. These observations corroborate the importance of the arylpiperazine fragment as potential target for molecular modification and further SAR studies, since this fragment has been strongly associated with 5-HT$_{1A}$ receptor affinity.

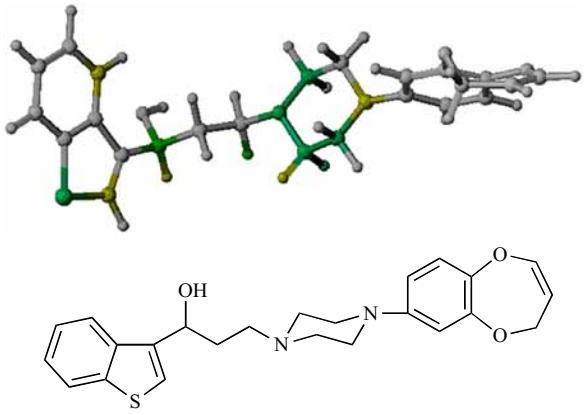

Fig. (3). Atomic contribution map for compound **65** of the data set.

4. CONCLUSIONS

In this work, 2D HQSAR models possessing both good internal and external consistency were generated for a large series of 5-HT$_{1A}$ ligands. The resulting HQSAR model is statistically robust with good correlative and predictive power. As the structure encoded within a molecular hologram is directly related to the biological activity of molecules within the data set, the generated HQSAR model can be used to predict 5-HT$_{1A}$ receptor affinities of new molecules from their molecular holograms. Therefore, the HQSAR model and the information obtained from 2D contribution maps should be useful for the design of new structurally related ligands of the 5-HT$_{1A}$ receptor with improved affinity.

ACKNOWLEDGEMENTS

The authors would like to thank the financial support from FAPESP (The State of São Paulo Research Foundation) and CNPq (The National Council for Scientific and Technological Development), Brazil.

REFERENCES

[1] Ramboz, S.; Oosting, R.; Amara, D.A.; Kung, H.F.; Blier, P.; Mendelsohn, M.; Mann, J. J.; Brunner, D.; Hen, R. *Proc. Natl. Acad. Sci. USA*, **1998**, *95*, 14476.

[2] Rocha, B.A.; Scearce-Levie, K.; Lucas, J.J.; Hiroi, N.; Castanon, N.; Crabbe, J.C.; Nestler, E. J.; Hen, R. *Nature,* **1998**, *393*, 175.

[3] Heisler, L. K.; Chu, H.-M.; Brennan, T.J.; Danao, J.A.; Bajwa, P.; Parsons, L.H.; Tecott, L.H. *Proc. Natl. Acad. Sci. USA,* **1998**, *95*, 15049.

[4] Murphy, D.L.; Wichems, C.; Li, Q.; Heils, A. *Trends Pharmacol. Sci.,* **1999**, *20*, 246.

[5] Parsons, L.H.; Kerr, T.M.; Tecott, L.H. *J. Neurochem.,* **2001**, *77*, 607.
[6] Rutter, J.J.; Gundlah, C.; Auerbach, S.B. *Synapse,* **1995**, *20*, 225.
[7] Chaput, Y.; De Montygny, C.; Blier, P. *Naunyn Schmiedebergs Arch. Pharmacol*., **1986**, *333*, 342.
[8] Artigas, F.; Perez, V.; Alvarez, E. *Arch. Gen. Psychiatry,* **1994**, *51*, 248.
[9] Tome, M.B.; Cloninger, C.R.; Watson, J.P.; Isaac, M.T. *J. Affect. Disord.,* **1997**, *44*, 101.
[10] Perez, V.; Gilaberte, I.; Faries, D.; Alvarez, E.; Artigas, F. *Lancet,* **1997**, *349*, 1594.
[11] Perez, V.; Soler, J.; Puigdemont, D.; Alvarez, E.; Artigas, F. *Arch. Gen Psychiatry,* **1999**, *56*, 375.
[12] Stockmeier, C.A.; Shapiro, L.A.; Dilley, G.E.; Kolli, T.N.; Friedman, L.; Rajkowska, G. *J. Neurosci.,* **1998**, *18*, 7394.
[13] Strobel, A.; Gutknecht, L.; Rothe, C.; Reif, A.; Mossner, R.; Zeng, Y. *J. Neural. Transm.,* **2003**, *110,* 1445.
[14] Oficialdegui, A.M.; Martinez, J.; Pérez, S.; Heras, B.; Irurzun, M.; Palop, J.A.; Tordera, R.; Lasheras, B.; Del Rio, J.; Monge, A. *Il Farmaco,* **2000**, *55*, 345.
[15] Martínez-Esparza, J.; Pérez-Silanes, S.; Oficialdegui, A.M.; Heras, B.; Orús, L.; Villanueva, H.; Palop, J.A.; Roca, J.; Mourelle, M.; Bosch, A.; Del Castillo, J.C.; Lasheras, B.; Tordera, R.; Del Rio, J.; Monge, A. *Eur. J. Med. Chem.,* **2001**, *36*, 55.
[16] Martínez-Esparza, J.; Oficialdegui, A.M.; Pérez-Silanes, S.; Heras, B. B.; Orús, L.; Palop, J.A.; Lasheras, B.; Roca, J.; Mourelle, M.; Bosch, A.; Del Castillo, J.C.; Tordera, R.; Del Rio, J.; Monge, A. *J. Med. Chem.,* **2001**, *44*, 418.
[17] Orús, L.; Pérez-Silanes, S.; Oficialdegui, A.M.; Martínez-Esparza, J.; Del Castillo, J.C.; Mourelle, M.; Langer, T.; Guccione, S.; Donzella, G.; Krovat, E.M.; Poptodorov, K.; Lasheras, B.; Ballaz, S.; Hervíaz, I.; Tordera, R.; Del Rio, J.; Monge, A. *J. Med. Chem.,* **2002**, *45*, 4128.
[18] López-Rodríguez, M.L.; Morcillo, M.J.; Rovat, T.K.; Fernández, E.; Vicente, B.; Sanz, A. M.; Hernández, M. *J. Med. Chem.,* **1999**, *42*, 36.
[19] Heinrich, T.; Böttcher, H.; Gericke, R.; Bartoszyk, G.D.; Anzali, S.; Seyfried, C.A.; Greiner, H.E.; Van Amsterdam,C. *J. Med. Chem.,* **2004**, *47*, 4684.
[20] Gaillard, P.; Carrupt, P.-A.; Testa, B.; Schambel, P. *J. Med. Chem.,* **1996**, *39*, 126.
[21] Menziani, M.C.; de Benedetti, P.G.; Karelson, M. *Bioorg. Med. Chem.,* **1998**, *6*, 535.
[22] López-Rodríguez, M.L.; Morcillo, M.J.; Fernández, E.; Rosado, M.L.; Pardo, L.; Schaper, K.-J. *J. Med. Chem.,* **2001**, *44*, 198.
[23] Weber, K.C.; da Silva, A.B.F. *Eur. J. Med. Chem*., **2008**, *43*, 364.
[24] Debnath, B.; Samanta, S.; Naskar, S.K.; Roy, K.; Jha T. *Bioorg. Med. Chem. Lett*., **2003**, *13*, 2837.
[25] Sharma, B. K.; Singh, P.; Sharma, S. *J. Enz. Inhib. Med. Chem*., **2006**, *21*, 601.
[26] Lowis, D.R. HQSAR a new, highly predictive QSAR technique. http://www.tripos.com/AppNotes/HQSAR/hqsar.html
[27] Honório, K.M.; Andricopulo, A.D. Two-dimensional quantitative structure-activity relationships: Hologram QSAR. In *Current Methods in Medicinal Chemistry and Biological Physics*, Carlton A. Taft and Carlos H. T. P. Silva (Eds.), **2007**, Vol.1, p. 49-60.
[28] Honorio, K.M.; Garratt, R.C.; Andricopulo, A.D. *Bioorg. Med. Chem. Lett.,* **2005**, *15*, 3119.
[29] Castilho, M.; Postigo, M.P.; de Paula, C.B.V.; Montanari, C.A.; Oliva, G.; Andricopulo, A.D. *Bioorg. Med. Chem. Lett.,* **2006**, *14*, 516.
[30] Honorio, K.M.; Garratt, R.C.; Polikarpov, I.; Andricopulo, A.D. *Lett. Drug Des. Discov.,* **2006**, *3*, 261.
[31] Salum, L.B.; Polikarpov, I.P.; Andricopulo, A.D. *J. Mol. Graph. Modell.*, **2007**, *25*, 434.

Received: 14 November, 2007 **Revised: 26 April, 2008** **Accepted: 06 May, 2008**